


7-11-2011

Top Quark Rapidity Distribution and Forward-backward Asymmetry

Nikolaos Kidonakis

Kennesaw State University, nkidonak@kennesaw.edu

Follow this and additional works at: <https://digitalcommons.kennesaw.edu/facpubs>

 Part of the [Atomic, Molecular and Optical Physics Commons](#), and the [Elementary Particles and Fields and String Theory Commons](#)

Recommended Citation

Kidonakis N. 2011. Top quark rapidity distribution and forward-backward asymmetry. *Phys.Rev.D* 84(1):011504.

This Article is brought to you for free and open access by DigitalCommons@Kennesaw State University. It has been accepted for inclusion in Faculty Publications by an authorized administrator of DigitalCommons@Kennesaw State University. For more information, please contact digitalcommons@kennesaw.edu.

The top quark rapidity distribution and forward-backward asymmetry

Nikolaos Kidonakis

*Kennesaw State University, Physics #1202,
1000 Chastain Rd., Kennesaw, GA 30144-5591, USA*

Abstract

I present results for the top quark rapidity distribution at LHC and Tevatron energies, including higher-order corrections from threshold resummation. The next-to-next-to-leading-order (NNLO) soft-gluon corrections at next-to-next-to-leading-logarithm (NNLL) level are added to the NLO result. Theoretical predictions are shown for the rapidity distribution, including the scale dependence of the distributions. The forward-backward asymmetry at the Tevatron is also calculated.

1 Introduction

The study of the top quark has a central role in current collider physics research programs. The experimental measurements of the $t\bar{t}$ quark cross section at the Tevatron [1, 2] and the LHC [3, 4], and of the top quark transverse momentum distribution at the Tevatron [5, 6] are currently in good agreement with theoretical predictions [7, 8]. The rapidity distribution and the forward-backward asymmetry (or charge asymmetry) have also been measured at the Tevatron [9, 10]. The forward-backward asymmetry has been found to be surprisingly large. This apparent discrepancy with theory, as well as the fact that experimental errors continue to get smaller, make precise theoretical calculations in the Standard Model necessary, in order to be able to clearly identify any effects of new physics.

Next-to-leading order (NLO) calculations of the QCD corrections to $t\bar{t}$ production have been available for over two decades [11, 12] but the associated uncertainty is much bigger than current experimental errors for the total cross section. The inclusion of higher-order soft-gluon corrections enhances the cross section and transverse momentum distribution and significantly reduces the theoretical error [7].

Recent theoretical predictions use approximate next-to-next-to-leading order (NNLO) calculations based on next-to-next-to-leading-logarithm (NNLL) resummation of soft-gluon corrections for the differential cross section [7]. To achieve NNLL accuracy in the resummation we have calculated the soft anomalous dimensions at two loops [7, 13, 14]. These soft-gluon corrections dominate the cross section for $t\bar{t}$ production and at first-order they provide an excellent approximation to the exact NLO corrections at both Tevatron and LHC energies [7, 8].

We begin with the double differential cross section, $d^2\sigma/(dp_T^2 dY)$, where p_T is the transverse momentum of the top quark, and Y is the rapidity of the top quark in the hadronic center-of-mass frame. We use our resummation formalism to calculate soft-gluon contributions for this differential cross section (see [7] and references therein). The total cross section was calculated in [7] by integrating over both p_T and rapidity. In [7] the p_T distribution, $d\sigma/dp_T$ was also calculated by integrating the double differential cross section over rapidity.

In this paper we calculate the rapidity distribution, $d\sigma/dY$, by integrating the double differential cross section over the transverse momentum

$$\frac{d\sigma}{dY} = \int_0^{p_{T+}^2} \frac{d^2\sigma}{dp_T^2 dY} dp_T^2 \quad (1.1)$$

where the upper limit of integration is $p_{T+}^2 = S/(4 \cosh^2 Y) - m^2$, with m the top quark mass and S the squared hadronic center-of-mass energy. The total cross section can also be calculated by integrating Eq. (1.1) over Y with integration limits $\pm(1/2) \ln[(1 + \beta)/(1 - \beta)]$ where $\beta = \sqrt{1 - 4m^2/S}$, which serves as a further check on the calculation.

In the next Section, we calculate the rapidity distribution at the LHC at 7 and 14 TeV energy while in Section 3 we do the calculation for Tevatron energy. In Section 4 we discuss the top quark forward-backward asymmetry at the Tevatron. We conclude in Section 5.

2 Top quark rapidity distribution at the LHC

We begin with a study of the top quark rapidity distribution at the LHC. We show results for the current LHC energy of 7 TeV and the future (design) energy of 14 TeV. We present NLO and approximate NNLO calculations for the rapidity distribution. The NNLO approximate rapidity distribution is computed by adding the NNLO soft-gluon corrections, derived from NNLL resummation, to the exact NLO result. In our calculations we use the MSTW2008 NNLO parton distribution functions [15].

The top quark rapidity distribution at the LHC at 7 TeV energy is plotted in Figs. 1 and 2. We use $m = 173$ GeV, currently the best value for the top quark mass [16]. We denote by μ the common factorization and renormalization scale. Fig. 1 shows NLO and approximate NNLO results for the differential distribution $d\sigma/dY$ for three different scale choices, $\mu = m/2$, m , and $2m$. The scale variation of the Y distribution at NNLO is much smaller than that at NLO, consistent with the results in Ref. [7] for the total cross section and p_T distribution.

Figure 2 presents the results at 7 TeV for $d\sigma/dY$ in a logarithmic plot for a wider range of rapidity values. It is clear that $d\sigma/dY$ falls off very quickly for larger rapidities. From both Figs. 1 and 2 we see that the NNLO soft-gluon corrections contribute an enhancement to the NLO rapidity distribution, but the shapes of the NLO and approximate NNLO distributions are similar.

The rapidity distribution of the top quark with $m = 173$ GeV at the LHC at 14 TeV energy is plotted in Figs. 3 and 4. Fig. 3 shows NLO and approximate NNLO results for three different scale choices, $\mu = m/2$, m , and $2m$. Again, the scale variation of the Y distribution at NNLO is much smaller than that at NLO.

Figure 4 presents the results for $d\sigma/dY$ at 14 TeV in a logarithmic plot for a wider range of Y values. The rapidity ranges shown in Figs. 3 and 4 are of course wider than the corresponding ones in Figs. 1 and 2, since the rate increases significantly at the higher energy. At 14 TeV the NNLO soft-gluon corrections provide a significant contribution, but the shapes of the NLO and the approximate NNLO distributions are similar.

In all four figures we see that the rapidity distributions at the LHC are fairly symmetric. This is due to the fact that the $gg \rightarrow t\bar{t}$ channel is dominant at the LHC, and this channel is completely symmetric at all orders. We discuss this in more detail in Section 4.

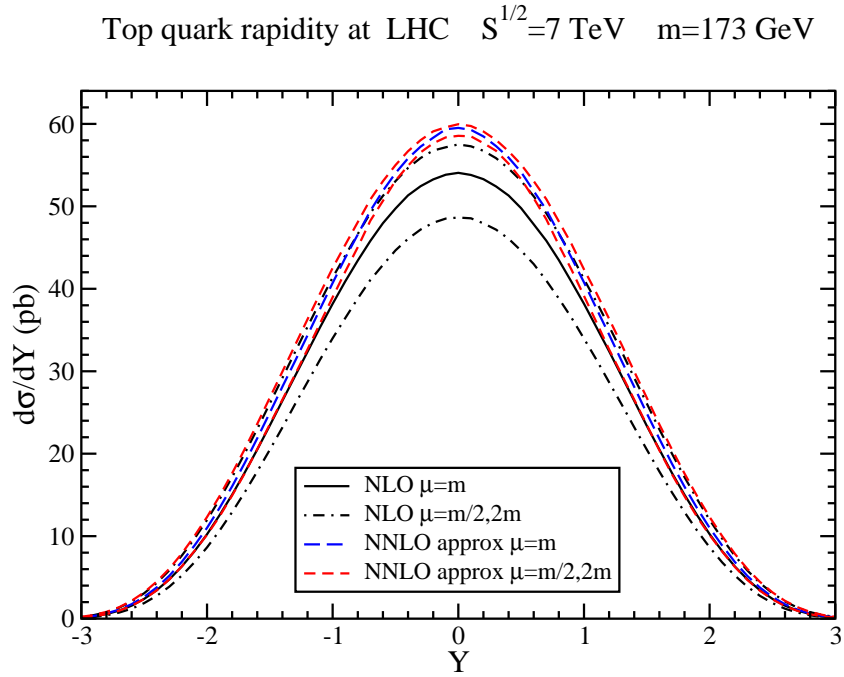


Figure 1: The top quark rapidity distribution at the LHC with $\sqrt{S} = 7$ TeV, $m = 173$ GeV, and $\mu = m/2, m, 2m$.

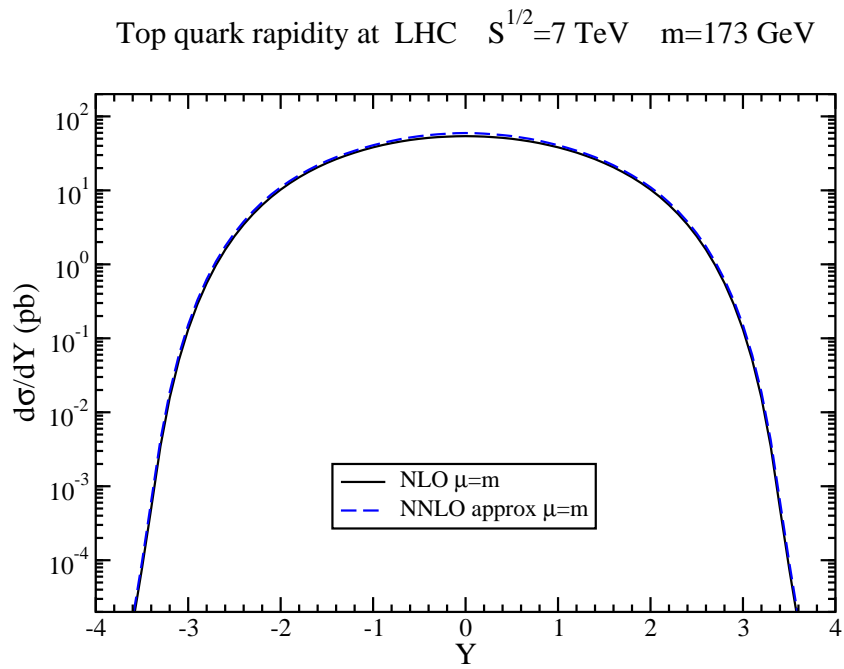


Figure 2: The top quark rapidity distribution at the LHC with $\sqrt{S} = 7$ TeV and $\mu = m = 173$ GeV in a logarithmic plot.

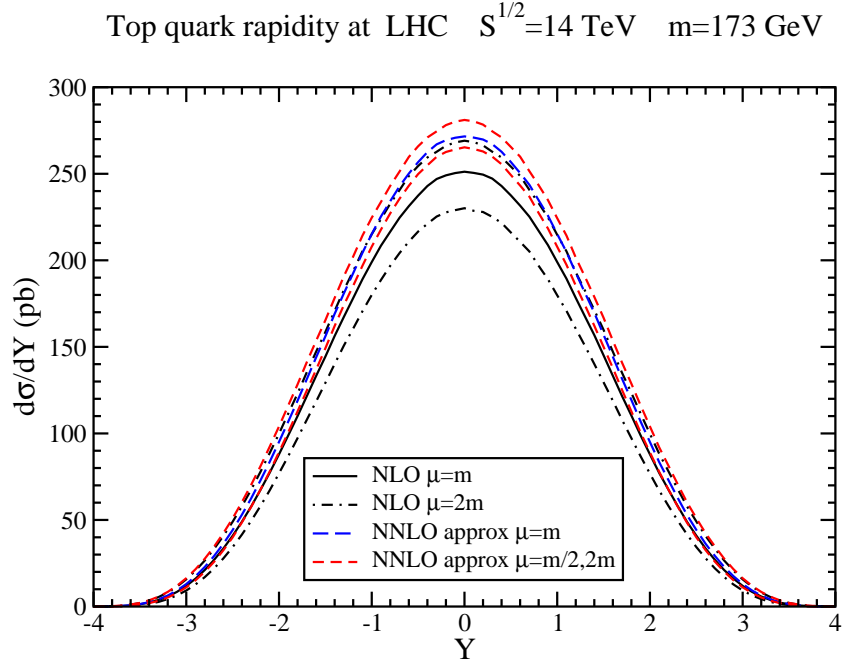


Figure 3: The top quark rapidity distribution at the LHC with $\sqrt{S} = 14$ TeV, $m = 173$ GeV, and $\mu = m/2, m, 2m$.

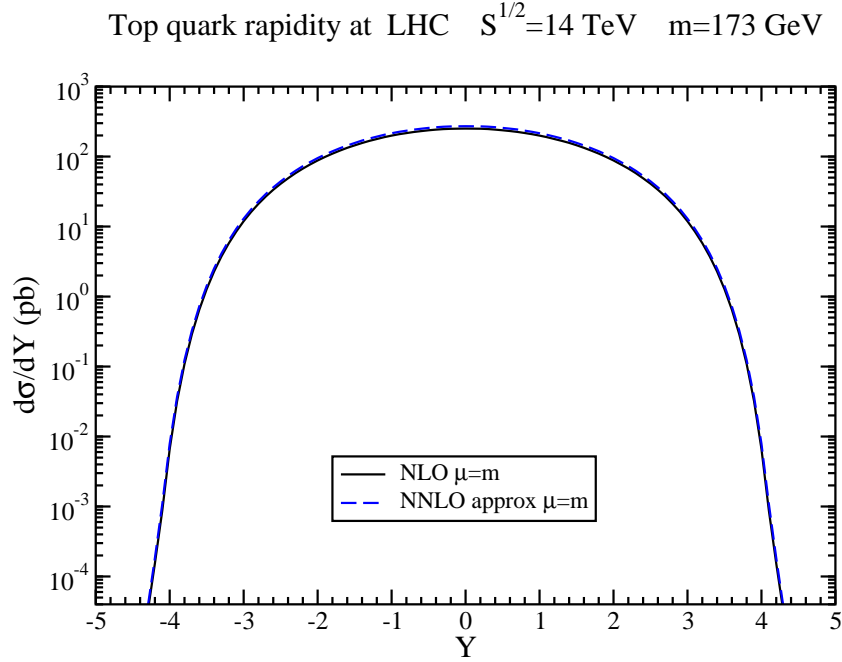


Figure 4: The top quark rapidity distribution at the LHC with $\sqrt{S} = 14$ TeV and $\mu = m = 173$ GeV in a logarithmic plot.

Top quark rapidity at Tevatron $S^{1/2}=1.96$ TeV $m=173$ GeV

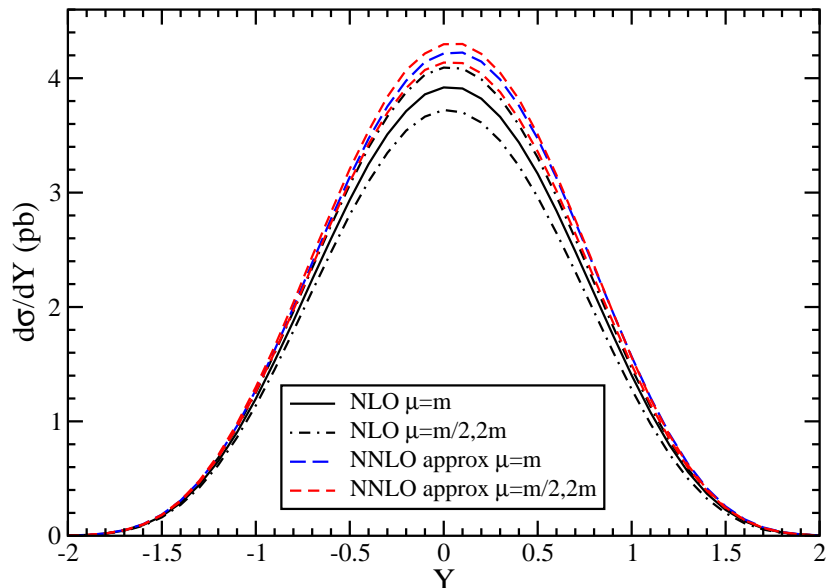


Figure 5: The top quark rapidity distribution at the Tevatron with $\sqrt{S} = 1.96$ TeV, $m = 173$ GeV, and $\mu = m/2, m, 2m$.

Finally, we note that the integrated rapidity distribution gives the same result for the total cross section as found in [7] at both LHC energies, which provides a good consistency check of the calculation.

3 Top quark rapidity distribution at the Tevatron

We continue with the top quark rapidity distribution at the Tevatron collider. Again, we present exact NLO and approximate NNLO (from NNLL resummation) results.

The top quark rapidity distribution at the Tevatron with $m = 173$ GeV is plotted in Figs. 5 and 6. Fig. 5 shows the differential distribution $d\sigma/dY$ at both NLO and approximate NNLO for three different scale choices, $\mu = m/2, m$, and $2m$. The integrated rapidity distribution gives the total cross section found in [7], which is a good consistency check of the calculation. The scale variation of the Y distribution at NNLO is significantly smaller than at NLO, again as also found for the total cross section and the p_T distribution in [7]. The NNLO soft-gluon corrections enhance the NLO result but the shape is not significantly affected.

Figure 6 presents the top quark rapidity distribution at the Tevatron in a logarithmic plot that makes it easier to see $d\sigma/dY$ for larger Y values. Again the fall of the distribution at larger Y is very steep.

We note that, unlike the LHC results, at the Tevatron the rapidity distribution of the top quark is clearly not symmetric. The maximum of the distribution is not at $Y = 0$ but at positive Y . We discuss this forward-backward asymmetry in the next Section.

Top quark rapidity at Tevatron $S^{1/2}=1.96$ TeV $m=173$ GeV

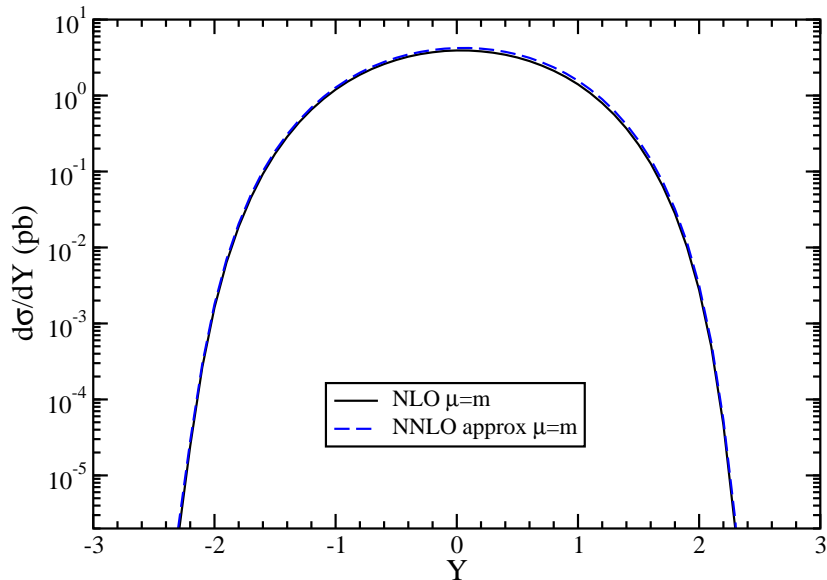


Figure 6: The top quark rapidity distribution at the Tevatron with $\sqrt{S} = 1.96$ TeV and $\mu = m = 173$ GeV in a logarithmic plot.

4 Top quark forward-backward asymmetry at the Tevatron

We define the top quark forward-backward asymmetry as

$$A_{FB} = \frac{\sigma(Y > 0) - \sigma(Y < 0)}{\sigma(Y > 0) + \sigma(Y < 0)}. \quad (4.1)$$

The asymmetry has been calculated in [17, 18, 19] in NLO QCD, and more recently using threshold resummation at NLL in [20] and using SCET at NNLL in [21].

The leading-order (LO) production channels, $q\bar{q} \rightarrow t\bar{t}$ and $gg \rightarrow t\bar{t}$, are symmetric in rapidity, thus A_{FB} vanishes at LO. The gg channel remains symmetric at all orders. However an asymmetry arises in the $q\bar{q}$ channel starting at NLO. Furthermore asymmetry arises from flavor excitation, $qg \rightarrow qt\bar{t}$ [11, 12, 17, 18, 19].

Therefore by applying resummation we expect the gg channel to remain symmetric, but we will have contributions to the asymmetry from higher orders in the $q\bar{q}$ channel. Since the gg channel is dominant at the LHC, the asymmetry there is very small, as can also be seen from the fairly symmetric rapidity distributions presented in Section 2. At the Tevatron, on the other hand, the $q\bar{q}$ channel is dominant and the asymmetry is larger and evident from the rapidity distributions presented in Section 3.

The measurements of A_{FB} at CDF [9] and D0 [10] have returned values substantially larger than the Standard Model prediction, so it is important to perform the most accurate calculation to have confidence in the theoretical prediction while seeking hints of new physics.

Using the NNLO approximate rapidity distributions in the previous section, we find a top quark forward-backward asymmetry at the Tevatron of 0.052, or 5.2%, in the $p\bar{p}$ center-of-mass frame. This is a modest increase on the 4% NLO asymmetry. Uncertainties on this number can be estimated by varying the scale μ between $m/2$ and $2m$ as shown for the rapidity distributions. The value of 0.052 found for $\mu = m$ is a maximum, but the number can vary down to 0.046 for $\mu = 2m$, so we write $A_{\text{FB}} = 0.052_{-0.006}^{+0.000}$. Current measurements at the Tevatron indicate asymmetries of 15% or more, with around two standard deviations excess over the theoretical prediction.

5 Conclusions

We have shown in this paper that the top quark rapidity distributions at the LHC and the Tevatron receive significant enhancements from soft-gluon corrections. These corrections have been resummed at NNLL accuracy by using the two-loop soft anomalous dimension matrices for the partonic processes. Approximate NNLO rapidity distributions have been derived from the NNLL resummed result. The NNLO soft-gluon corrections enhance the top quark rapidity distribution and greatly reduce the theoretical uncertainty from scale variation. The top quark forward-backward asymmetry at the Tevatron has been calculated. The theoretical prediction of 5.2% is significantly smaller than current experimental values.

Acknowledgements

This work was supported by the National Science Foundation under Grant No. PHY 0855421.

References

- [1] CDF Collaboration, T. Aaltonen *et al.*, Phys. Rev. D **79**, 052007 (2009) [arXiv:0901.4142 [hep-ex]]; Phys. Rev. D **79**, 112007 (2009) [arXiv:0903.5263 [hep-ex]]; Phys. Rev. D **81**, 052011 (2010) [arXiv:1002.0365 [hep-ex]]; Phys. Rev. D **82**, 052002 (2010) [arXiv:1002.2919 [hep-ex]]; Phys. Rev. D **81**, 092002 (2010) [arXiv:1002.3783 [hep-ex]]; Phys. Rev. D **83**, 071102 (2011) [arXiv:1007.4423 [hep-ex]]; arXiv:1103.4821 [hep-ex]; arXiv:1105.1806 [hep-ex]; Conf. Note 9913.
- [2] D0 Collaboration, V.M. Abazov *et al.*, Phys. Rev. Lett. **100**, 192003 (2008) [arXiv:0801.1326 [hep-ex]]; Phys. Rev. Lett. **100**, 192004 (2008) [arXiv:0803.2779 [hep-ex]]; Phys. Lett. B **679**, 177 (2009) [arXiv:0901.2137 [hep-ex]]; Phys. Rev. D **80**, 071102 (2009) [arXiv:0903.5525 [hep-ex]]; Phys. Rev. D **82**, 032002 (2010) [arXiv:0911.4286 [hep-ex]]; Phys. Rev. D **82**, 071102 (2010) [arXiv:1008.4284 [hep-ex]]; arXiv:1101.0124 [hep-ex]; arXiv:1104.2887 [hep-ex].
- [3] ATLAS Collaboration, G. Aad *et al.*, Eur. Phys. J. C **71**, 1577 (2011) [arXiv:1012.1792 [hep-ex]]; ATLAS-CONF-2011-040; ATLAS-CONF-2011-054.

- [4] CMS Collaboration, V. Khachatryan *et al.*, Phys. Lett. B **695**, 424 (2011) [arXiv:1010.5994 [hep-ex]]; CMS-PAS-TOP-11-001.
- [5] CDF Collaboration, A.A. Affolder *et al.*, Phys. Rev. Lett. **87**, 102001 (2001); CDF II Collaboration, CDF Note 10234.
- [6] D0 Collaboration, V.M. Abazov *et al.*, Phys. Lett. B **693**, 515 (2010) [arXiv:1001.1900 [hep-ex]].
- [7] N. Kidonakis, Phys. Rev. D **82**, 114030 (2010) [arXiv:1009.4935 [hep-ph]].
- [8] N. Kidonakis, in *DIS 2011*, arXiv:1105.3481 [hep-ph].
- [9] CDF Collaboration, T. Aaltonen *et al.*, Phys. Rev. Lett. **101**, 202001 (2008) [arXiv:0806.2472 [hep-ex]]; CDF Note 9724; 9853; 10224; 10436; arXiv:1101.0034 [hep-ex].
- [10] D0 Collaboration, V.M. Abazov *et al.*, Phys. Rev. Lett. **100**, 142002 (2008) [arXiv:0712.0851 [hep-ex]]; D0 Note 6062-CONF.
- [11] P. Nason, S. Dawson, and R.K. Ellis, Nucl. Phys. B **303**, 607 (1988); Nucl. Phys. **327**, 49 (1989); (E) B **335**, 260 (1990).
- [12] W. Beenakker, H. Kuijf, W.L. van Neerven, and J. Smith, Phys. Rev. D **40**, 54 (1989); W. Beenakker, W.L. van Neerven, R. Meng, G.A. Schuler, and J. Smith, Nucl. Phys. B **351**, 507 (1991).
- [13] N. Kidonakis, Phys. Rev. Lett. **102**, 232003 (2009) [arXiv:0903.2561 [hep-ph]].
- [14] N. Kidonakis, Phys. Rev. D **81**, 054028 (2010) [arXiv:1001.5034 [hep-ph]]; Phys. Rev. D **82**, 054018 (2010) [arXiv:1005.4451 [hep-ph]]; Phys. Rev. D **83**, 091503(R) (2011) [arXiv:1103.2792 [hep-ph]].
- [15] A.D. Martin, W.J. Stirling, R.S. Thorne, and G. Watt, Eur. Phys. J. C **63**, 189 (2009) [arXiv:0901.0002 [hep-ph]].
- [16] Tevatron Electroweak Working Group, arXiv:1007.3178.
- [17] F. Halzen, P. Hoyer, and C.S. Kim, Phys. Lett. B **195**, 74 (1987).
- [18] J.H. Kuhn and G. Rodrigo, Phys. Rev. Lett. **81**, 49 (1998) [hep-ph/9802268]; Phys. Rev. D **59**, 054017 (1999) [hep-ph/9807420].
- [19] M.T. Bowen, S.D. Ellis, and D. Rainwater, Phys. Rev. D **73**, 014008 (2006) [hep-ph/0509267].
- [20] L.G. Almeida, G. Sterman, and W. Vogelsang, Phys. Rev. D **78**, 014008 (2008) [arXiv:0805.1885 [hep-ph]].
- [21] V. Ahrens, A. Ferroglia, M. Neubert, B.D. Pecjak, and L.L. Yang, arXiv:1103.0550 [hep-ph].